Benchmarking electronic-state excitation cross sections for electron-N_2 collisions

Hidetoshi Kato, Daisuke Suzuki, Mizuha Ohkawa, Masamitsu Hoshino, and Hiroshi Tanaka
Department of Physics, Sophia University, Chiyoda-ku, Tokyo 102-8554, Japan

Laurence Campbell and Michael J. Brunger
Australian Research Council Centre for Antimatter-Matter Studies, School of Chemical and Physical Sciences, Flinders University, General Post Office Box 2100, Adelaide, South Australia 5001, Australia

(Received 23 February 2010; published 30 April 2010)

We report differential cross sections for electron impact excitation of the $a\,^1\Pi_g$, $C\,^3\Pi_u$, $E\,^3\Sigma_g^+$, $a''\,^1\Sigma_g^+$, $b\,^1\Pi_u$, $c_3\,^1\Pi_u$, $o_3\,^1\Pi_u$, $b'\,^1\Sigma_u^+$, $c_4'\,^1\Sigma_u^+$, $G\,^3\Pi_u$, and $F\,^3\Pi_u$ electronic states in N_2. The incident electron energies are 20, 30, and 40 eV, while the scattered electron angles are 10° and 20°. These kinematic conditions were specifically targeted in order to try and shed new light on the worrying discrepancies that exist in the literature for the $a\,^1\Pi_g$, $C\,^3\Pi_u$, $E\,^3\Sigma_g^+$, and $a''\,^1\Sigma_g^+$ cross sections, and in general the present measurements confirm that those from the more recent results of the University of California, Fullerton, and the Jet Propulsion Laboratory [M. A. Khakoo, P. V. Johnson, I. Ozkay, P. Yan, S. Trajmar, and I. Kanik, Phys. Rev. A **71**, 062703 (2005); C. P. Malone, P. V. Johnson, I. Kanik, B. Ajdari, and M. A. Khakoo, Phys. Rev. A **79**, 032704 (2009)] are reliable. In addition, we provide a rigorous cross-check for the remaining seven electronic states, where the only recent comprehensive study is from Khakoo and colleagues [Phys. Rev. A **77**, 012704 (2008)]. Here, however, some of those cross sections are confirmed and others are not, suggesting that further work is still needed.

DOI: 10.1103/PhysRevA.81.042717 PACS number(s): 34.50.Gb

I. INTRODUCTION

Molecular nitrogen (N_2) is a major constituent of Earth's atmosphere, so to obtain a quantitative understanding of the atmospheric behavior of our planet, the role of electron-driven processes is an important component [1–3]. As a part of this, electron impact excitation of the electronic states in N_2 is particularly interesting as it leads to a wealth of atmospheric emission lines [4,5]. In addition, laboratory-based discharge experiments, in which N_2 is a component, can also only be understood if a detailed knowledge of those electronic-state excitation cross sections is available [6].

It is therefore not surprising that significant effort, particularly at the Jet Propulsion Laboratory (JPL) and also more recently at the Fullerton campus of the University of California [7–15], has gone into measuring differential cross sections (DCSs) and integral cross sections for the electron impact excitation of the electronic states in N_2. A summary of the early results can be found in Ref. [16], while those from the more recent measurements are detailed in the JPL/Fullerton papers [11–15]. Unfortunately, despite all these endeavors, if we were to characterize the level of agreement between these studies, over the common energy, angular range, or both, for the 17 lower-lying N_2 electronic states, then we could only conclude that it remains "patchy" at best. There are probably three main reasons for this situation. First, even though N_2 is a homonuclear diatomic molecule, its spectroscopy is rather complicated [14,17], with many of the vibrational sublevels of a given electronic state overlapping with other vibrational sublevels of different electronic states (see Fig. 1). Given that the energy resolution of most of the electron spectrometers employed to make these DCS measurements is typically between 30 and 60 meV, this makes the spectral deconvolution of the measured energy-loss spectra somewhat problematic for deriving unique results. Rydberg-valence interactions [14] between the higher-lying electronic states and the breakdown [14,15] of the Franck-Condon approximation further complicate the interpretation. A second possible problem, particularly with the older data, is whether or not the scattered electron analyzer transmission function, over the quite large energy-loss range being considered, is appropriately characterized. If not, then systematic errors would be introduced into the derived cross sections. However, a recent protocol from Allan [18], if correctly applied, should now ensure the response is correctly calibrated to about the 20% level. Finally, and again this is now largely historical, different groups employed different procedures and reference cross sections [16] to normalize their measured (relative) energy-loss spectra to an absolute scale. Today, however, there is a fairly good consensus as to the absolute elastic-helium and elastic-N_2 DCSs that might be employed in such a normalization (see also Sec. II).

From a theoretical perspective, the available calculations and a comparison of those theories with experimental data can be found in Ref. [16]. Subsequent to that review, we also note the more recent Schwinger multichannel variational results from da Costa and Lima [19,20]. Nonetheless, due to difficulties both in getting an accurate target state description as well as in performing what are very complex scattering computations, the theory is not yet at a stage where it could be used to benchmark the available experimental data.

We therefore report results from a very specific series of DCS measurements, which in no way attempt to mimic the comprehensive studies already available in the literature [7–9,11–15,17,21]. Rather, here we target various topical kinematic conditions in order to try and shed new light on the discrepancies between the available DCS data for the $a\,^1\Pi_g$, $C\,^3\Pi_u$, $E\,^3\Sigma_g^+$, and $a''\,^1\Sigma_g^+$ states. We do so in order to give guidance to the modeling communities, so that they can select the best available Atomic, Molecular and Optical Physics (ATMOP) data for their environmentally or industrially related

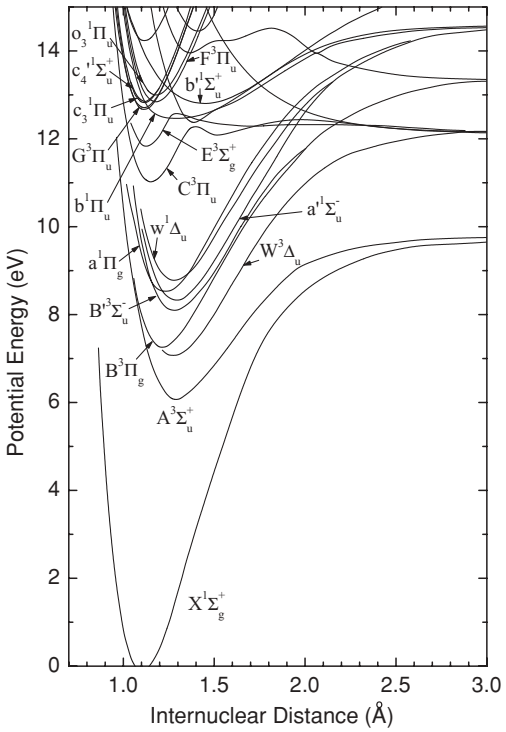

FIG. 1. Potential energy versus internuclear separation curves for 16 of the 17 lowest-lying electronic states in N_2. This figure clearly indicates the complex spectroscopy of the N_2 molecule.

simulations. In addition, we also provide DCSs for the $b\,^1\Pi_u$, $c_3\,^1\Pi_u$, $o_3\,^1\Pi_u$, $b'\,^1\Sigma_u^+$, $c_4'\,^1\Sigma_u^+$, $G\,^3\Pi_u$, and $F\,^3\Pi_u$ electronic states in order to benchmark the comprehensive results of Khakoo *et al.* [14] and the original measurements by Chutjian *et al.* [9]. In Sec. II we briefly describe our apparatus and measurement procedures as well as our spectral deconvolution technique. In Sec. III we then present the results from this study and a discussion of those results, before finishing with some conclusions that we draw from this investigation.

II. EXPERIMENTAL DETAILS AND ANALYSIS TECHNIQUES

A. Differential cross-section measurements

The present spectrometer [22] consists of an electron gun with a hemispherical monochromator, a molecular beam crossed at right angles to the incident electrons, and a rotatable detector ($\theta = -10°$–$130°$) with a second hemispherical analyzer system. A number of electron optic elements image and energy-control the electron beam, and their performance was checked by detailed electron trajectory calculations. Both the monochromator and the analyzer are housed in differentially pumped boxes in order to reduce the effect of any background gases and to minimize the stray electron background. The target molecular beam is produced by effusing N_2 through a simple nozzle with an internal diameter of 0.3 mm and a length of 5 mm.

The incident electron energies (E_0) of the present study were 20, 30, and 40 eV, and the scattered electron angles (θ_{sc}) were 10° and 20°. In all of these cases the energy resolution

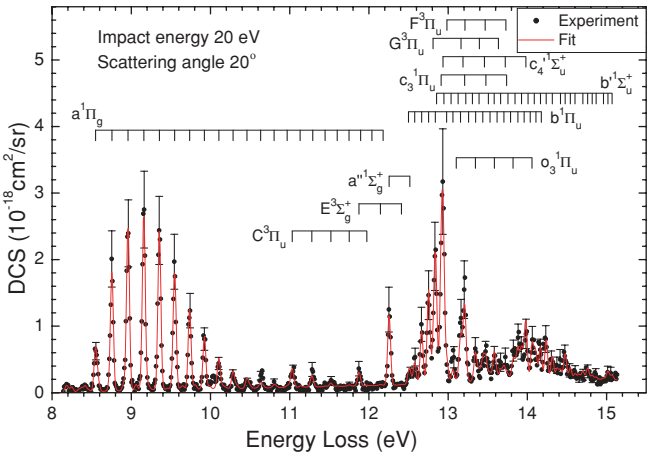

FIG. 2. (Color online) Typical energy-loss spectrum for electron impact excitation of the relevant electronic states of N_2, at an impact energy of 20 eV and a scattering angle of 20°. Also shown is our spectral deconvolution of this energy-loss spectrum and the various vibrational sublevels of each electronic state.

was in the range 35–40 meV [full width at half maximum (FWHM)] and the angular resolution was $\sim\pm1.5°$ (FWHM). The primary electron beam current was typically in the range 3–5 nA. The incident electron energy was calibrated with respect to the 19.37-eV resonance of He [23].

Electron energy loss spectra (EELS) were measured, at each incident electron energy and each scattered electron angle, over the energy-loss range encompassing the elastic peak and from 8.2 to 15.2 eV. A typical example of these data at $E_0 = 20$ eV and $\theta_{sc} = 20°$ is shown in Fig. 2, where we note that the elastic peak has been suppressed for the sake of clarity. The absolute scales (see the y axis) of the present energy-loss spectra were set using the relative flow technique [24] with helium elastic DCSs as the standard [25]. Note that, for each of the 11 electronic states, it is the sum of the areas under each of the energy-loss peaks for all vibrational sublevels that sets their respective manifold differential cross sections for the incident electron energy and electron scattering angle in question. For the incident energies of interest ($E_0 = 20$–40 eV) and the energy-loss range of interest ($\Delta E = 8.2$–15.2 eV), the ratio of the energy loss to the incident energy varies roughly in the range $0.2 < \Delta E/E_0 < 0.76$. Thus, it is crucial to establish the transmission of the analyzer over this energy-loss range, with our procedure for doing so being found in Ref. [26]. We also note the approach of Allan [18] in this regard.

Experimental errors in the present DCSs are estimated at about 20–30% and include components due to the uncertainty in our analyzer transmission response, an uncertainty due to errors associated with the elastic normalization cross sections, uncertainties due to any fluctuations in target density and/or the incident electron beam current during the measurements, and an uncertainty associated with the spectral deconvolution process that we now discuss.

B. Spectral deconvolution of the present EELS

The fitting procedure has been described in detail earlier [27]. The input data are the energies and Franck-Condon factors for all known levels of all component states. These

TABLE I. DCS (10^{-18} cm^2/sr) for electron impact excitation of the present 11 electronic states of N_2. The percentage uncertainties of the DCS are given in parentheses.

Impact energy (eV)	Scattering angle (deg)	DCS (10^{-18} cm^2/sr)					
		$a\,^1\Pi_g$	$C\,^3\Pi_u$	$E\,^3\Sigma_g^+$	$a''\,^1\Sigma_g^+$	$b\,^1\Pi_u$	$c_3\,^1\Pi_u$
20	20	14.691(±25%)	0.515(±30%)	0.229(±30%)	1.239(±29%)	7.446(±27%)	2.714(±28%)
30	10	16.104(±25%)		0.252(±30%)	3.788(±28%)	36.058(±23%)	14.285(±25%)
30	20	11.302(±26%)	0.1488(±33%)	0.118(±33%)	0.336(±30%)	20.827(±24%)	7.222(±27%)
40	10	11.903(±25%)	0.1554(±33%)	0.160(±33%)	2.936(±28%)	44.807(±22%)	18.803(±24%)
40	20	8.845(±27%)	0.1245(±33%)		0.101(±33%)	16.115(±25%)	6.041(±27%)

Impact energy (eV)	Scattering angle (deg)	DCS (10^{-18} cm^2/sr)				
		$o_3\,^1\Pi_u$	$b'\,^1\Sigma_u^+$	$c_4'\,^1\Sigma_u^+$	$G\,^3\Pi_u$	$F\,^3\Pi_u$
20	20	1.333(±29%)	5.025(±27%)	3.077(±28%)	0.5554(±30%)	0.4516(±30%)
30	10	8.700(±27%)	35.159(±23%)	23.016(±24%)	1.698(±29%)	0.874(±30%)
30	20	4.614(±28%)	20.293(±24%)	8.492(±27%)	0.519(±30%)	0.816(±30%)
40	10	10.479(±26%)	47.932(±22%)	27.887(±23%)	1.569(±29%)	2.099(±28%)
40	20	3.287(±28%)	14.773(±25%)	5.189(±27%)	0.564(±30%)	0.689(±30%)

lines are convolved with a Gaussian shape and entered in multiparameter fits to the five experimental spectra, using the Marquardt method of least-squares fitting [28], to find the optimum combination of intensities of all states and the width of the Gaussian function.

Energy levels, and Franck-Condon factors or relative intensities, were acquired from four references. The values used for each level were the first found by consulting these references in the following order: energies and relative excitation probabilities given by Khakoo *et al.* [14], energies and Franck-Condon factors given by Gilmore *et al.* [29], energies and relative intensities given by Joyez *et al.* [30], and finally energies given by Stahel *et al.* [31]. For the states $c_4'\,^1\Sigma_u^+$, $b'\,^1\Sigma_u^+$, $b\,^1\Pi_u$, $o_3\,^1\Pi_u$, and $e'\,^1\Sigma_g^+$, one or more of the upper levels were not detailed in the first three references, while for the $E\,^3\Sigma_g^+$ state, level 2 was not specified by Gilmore *et al.* and so the energy was taken from Joyez *et al.* For these six states, the extra upper levels were initially treated as separate states in the fits to the five experimental spectra. This gave fitted intensities for each of the individual higher levels relative to a single fitted value for the set of lower levels for which Franck-Condon factors or relative intensities were specified. All these fitted intensities for each state were then normalized to produce a hybrid set of Franck-Condon factors for that state, for each experimental spectrum. These results were then averaged, to produce sets of pseudo-Franck-Condon factors that are independent of angle and energy. The fitting procedure (including all states) was then run again using these hybrid sets of Franck-Condon factors for the six states listed above, with the outcome that the individual-state and manifold differential cross sections, at each incident electron energy and scattering angle, were determined for the 11 electronic states of interest to this study. We note that the end result of this approach is actually quite consistent with that adopted in the work of Khakoo *et al.* [14]. A typical result from this procedure is given in Fig. 2, where it is seen that the experimental data and synthesized spectrum are in very good accord.

III. RESULTS AND DISCUSSION

In Table I we present our new DCS data at $E_0 = 20$, 30, and 40 eV, and at $\theta_{sc} = 10^\circ$ and 20°, for electron impact excitation of the $a\,^1\Pi_g$, $C\,^3\Pi_u$, $E\,^3\Sigma_g^+$, $a''\,^1\Sigma_g^+$, $b\,^1\Pi_u$, $c_3\,^1\Pi_u$, $o_3\,^1\Pi_u$, $b'\,^1\Sigma_u^+$, $c_4'\,^1\Sigma_u^+$, $G\,^3\Pi_u$, and $F\,^3\Pi_u$ electronic states in N_2. These data are also shown in Figs. 3–8, and compared with the earlier results. Note that these figures show the energy dependence of the DCSs for each of the electronic excitation states and that the errors plotted represent the one-standard-deviation uncertainties of our results.

If we consider the DCS available in the literature ([7–17] and references therein) for the $a\,^1\Pi_g$, $C\,^3\Pi_u$, $E\,^3\Sigma_g^+$, and $a''\,^1\Sigma_g^+$ states, then in many cases where a disagreement between the respective data sets is found it is not so much in the shape of the cross sections (angular distributions) but rather in the absolute values. Hence, clarifying this controversy does not require a remeasurement of those entire angular distributions; it just needs a couple of "cross-check" DCSs to be measured at some well-chosen electron scattering angles. This is precisely what we have done in this study.

Examining Figs. 3(a) and 3(b) in more detail, for the $a\,^1\Pi_g$ electronic state, we find excellent agreement with the results of Khakoo *et al.* [11], and with the trend in the energy dependence of the DCS found by Khakoo *et al.* [11], at both scattering angles. We also clearly see that the data of Brunger and Teubner [17] do not fit the energy-dependent trend of the DCS very well, at 17.5 and 15 eV; their data are somewhat too high in magnitude. This effect is even more pronounced for the $C\,^3\Pi_u$ state, where the DCSs of Brunger and Teubner [17] are significantly higher in magnitude than the other measurements at the lower energies [see Figs. 3(c) and 3(d)]. In this case, there are two recent measurements from the JPL/Fullerton collaboration [11,15], with the present results supporting more those of Malone *et al.* [15] over those from Khakoo *et al.* [11]. This apparent discrepancy between the recent JPL data, however, can be easily understood by Malone *et al.* [15] taking

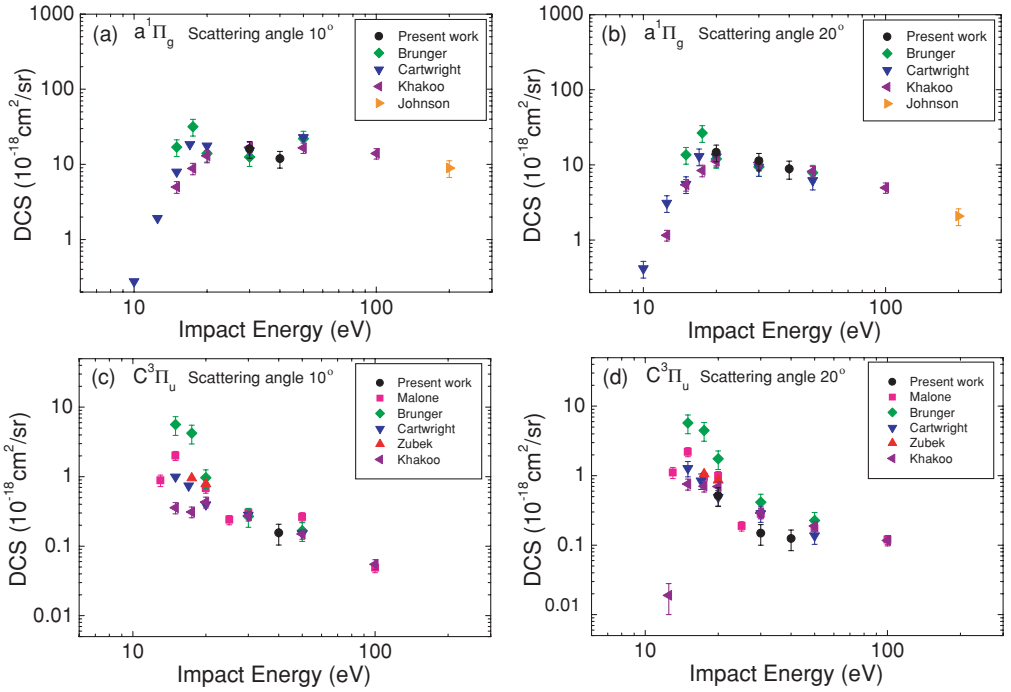

FIG. 3. (Color online) Energy dependence of the differential cross sections (10^{-18} cm^2/sr) for electron impact excitation of the $a\,^1\Pi_g$ and $C\,^3\Pi_u$ electronic states in N_2. Present $a\,^1\Pi_g$ data (●) at (a) $\theta_{sc} = 10^\circ$ and (b) $\theta_{sc} = 20^\circ$ are compared to the earlier results of Brunger and Teubner [17] (♦), Cartwright *et al.* [7] (▼), Khakoo *et al.* [11] (◄), and Johnson *et al.* [12] (►). Also the present $C\,^3\Pi_u$ data (●) at (c) $\theta_{sc} = 10^\circ$ and (d) $\theta_{sc} = 20^\circ$ are compared to the earlier results of Malone *et al.* [15] (■), Brunger and Teubner [17] (♦), Cartwright *et al.* [7] (▼), Zubek and King [21] (▲), and Khakoo *et al.* [11] (◄).

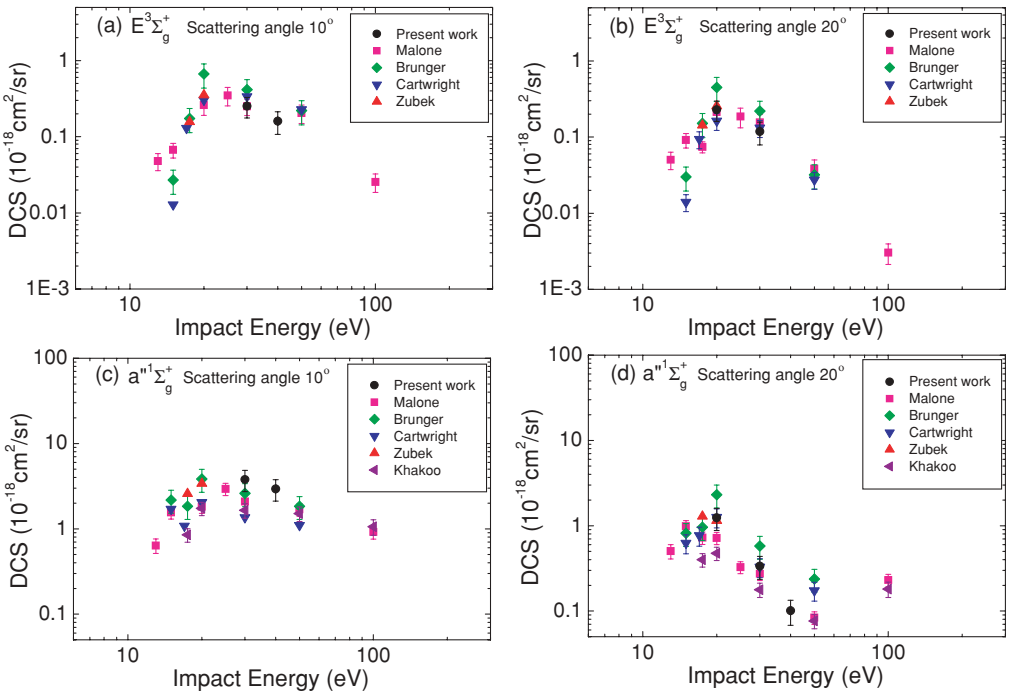

FIG. 4. (Color online) Energy dependence of the differential cross sections (10^{-18} cm^2/sr) for electron impact excitation of the $E\,^3\Sigma_g^+$ and $a''\,^1\Sigma_g^+$ electronic states in N_2. Present $E\,^3\Sigma_g^+$ data (●) at (a) $\theta_{sc} = 10^\circ$ and (b) $\theta_{sc} = 20^\circ$ are compared to the earlier results of Malone *et al.* [15] (■), Brunger and Teubner [17] (♦), Cartwright *et al.* [7] (▼) and Zubek and King [21] (▲). Also the present $a''\,^1\Sigma_g^+$ data (●) at (c) $\theta_{sc} = 10^\circ$ and (d) $\theta_{sc} = 20^\circ$ are compared to the earlier results of Malone *et al.* [15] (■), Brunger and Teubner [17] (♦), Cartwright *et al.* [7] (▼), Zubek and King [21] (▲), and Khakoo *et al.* [14] (◄).

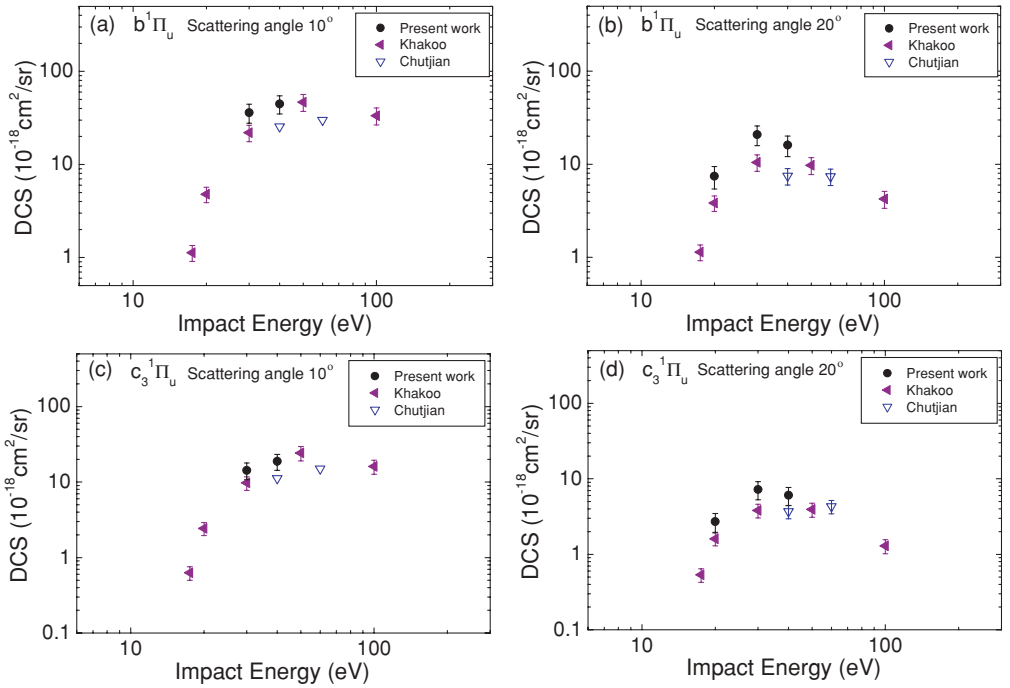

FIG. 5. (Color online) Energy dependence of the differential cross sections (10^{-18} cm^2/sr) for electron impact excitation of the $b\,^1\Pi_u$ and $c_3\,^1\Pi_u$ electronic states in N_2. Present $b\,^1\Pi_u$ data (●) at (a) $\theta_{sc} = 10^\circ$ and (b) $\theta_{sc} = 20^\circ$ are compared to the earlier results of Khakoo *et al.* [14] (◀) and Chutjian *et al.* [9] (▽). Also the present $c_3\,^1\Pi_u$ data (●) at (c) $\theta_{sc} = 10^\circ$ and (d) $\theta_{sc} = 20^\circ$ are compared to the earlier results of Khakoo *et al.* [14] (◀) and Chutjian *et al.* [9] (▽).

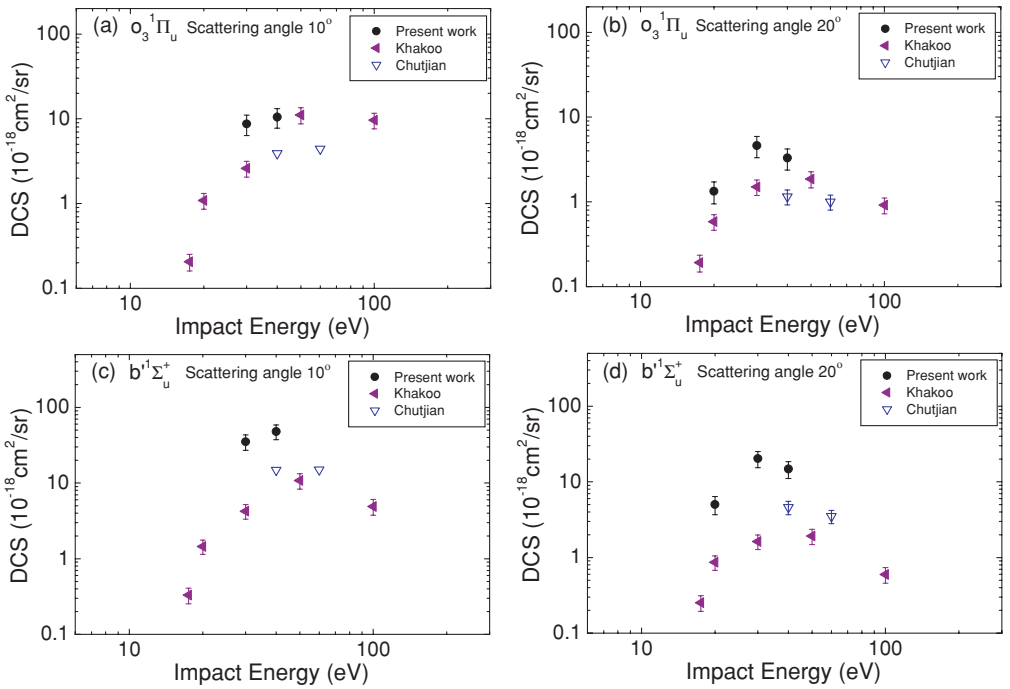

FIG. 6. (Color online) Energy dependence of the differential cross sections (10^{-18} cm^2/sr) for electron impact excitation of the $o_3\,^1\Pi_u$ and $b'\,^1\Sigma_u^+$ electronic states in N_2. Present $o_3\,^1\Pi_u$ data (●) at (a) $\theta_{sc} = 10^\circ$ and (b) $\theta_{sc} = 20^\circ$ are compared to the earlier results of Khakoo *et al.* [14] (◀) and Chutjian *et al.* [9] (▽). Also the present $b'\,^1\Sigma_u^+$ data (●) at (c) $\theta_{sc} = 10^\circ$ and (d) $\theta_{sc} = 20^\circ$ are compared to the earlier results of Khakoo *et al.* [14] (◀) and Chutjian *et al.* [9] (▽).

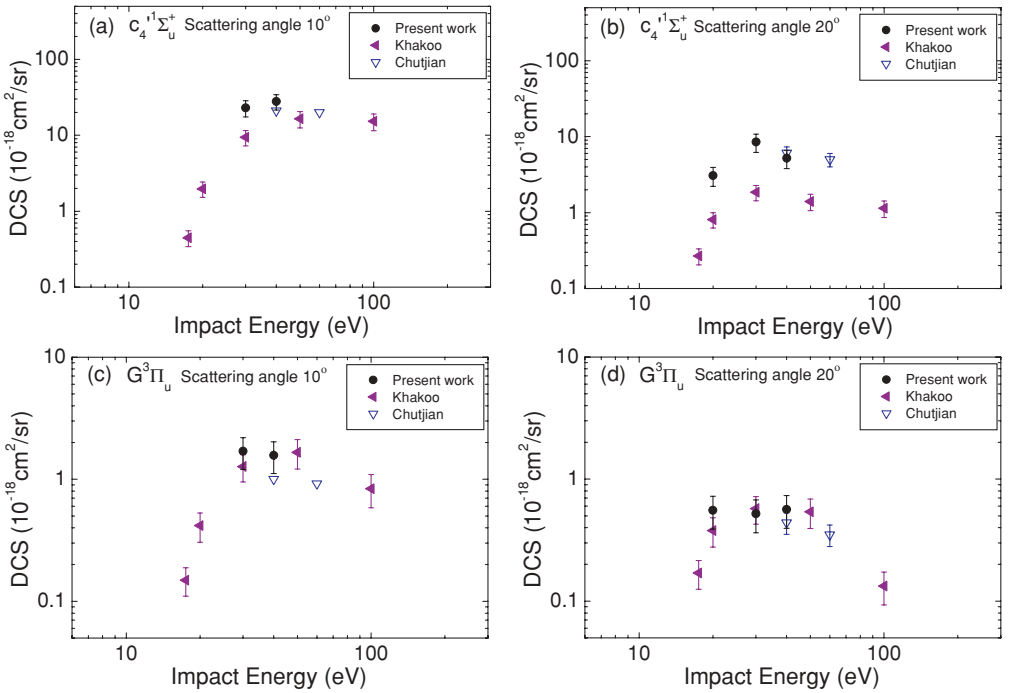

FIG. 7. (Color online) Energy dependence of the differential cross sections (10^{-18} cm^2/sr) for electron impact excitation of the $c_4'\,^1\Sigma_u^+$ and $G\,^3\Pi_u$ electronic states in N_2. Present $c_4'\,^1\Sigma_u^+$ data (●) at (a) $\theta_{sc} = 10^\circ$ and (b) $\theta_{sc} = 20^\circ$ are compared to the earlier results of Khakoo *et al.* [14] (◀) and Chutjian *et al.* [9] (▽). Also the present $G\,^3\Pi_u$ data (●) at (c) $\theta_{sc} = 10^\circ$ and (d) $\theta_{sc} = 20^\circ$ are compared to the earlier results of Khakoo *et al.* [14] (◀) and Chutjian *et al.* [9] (▽).

into account deviations from ideal Franck-Condon behavior in their analysis for this state, whereas Khakoo *et al.* [11] did not.

In Figs. 4(a) and 4(b) we see that the present $E\,^3\Sigma_g^+$ state DCSs are in excellent agreement with those of Malone *et al.* [15], for both angles, and they also fit well with the energy trends of the excitation functions. In this case, agreement with the data of Brunger and Teubner [17] and Zubek and King [21] is also satisfactory. For the $a''\,^1\Sigma_g^+$ electronic state [see Figs. 4(c) and 4(d)], we again somewhat favor the results of Malone *et al.* [15] over those of Khakoo *et al.* [11]; the present DCSs are also, to within the combined uncertainties, in fair accord with those of Brunger and Teubner [17] and Zubek and King [21]. There can be little doubt that the current data, as just presented in Figs. 3 and 4, help to clarify the controversies in the literature, where they exist, between the previous N_2 electronic state cross sections in favor of those from the JPL/Fullerton collaboration [11,15].

For the remaining $b\,^1\Pi_u$, $c_3\,^1\Pi_u$, $o_3\,^1\Pi_u$, $b'\,^1\Sigma_u^+$, $c_4'\,^1\Sigma_u^+$, $G\,^3\Pi_u$, and $F\,^3\Pi_u$ electronic states, the only cross sections currently available originate from either JPL [9] or JPL/Fullerton [14] and they are often in only marginal agreement with one another. All these data are plotted in Figs. 5–8, along with the present results. Considering, initially, Figs. 5 and 6, we find that the level of agreement between our results and those of Khakoo *et al.* [14], or in the energy trend of the results of Khakoo *et al.* [14], is typically very good for both the $b\,^1\Pi_u$ [Figs. 5(a) and 5(b)] and $c_3\,^1\Pi_u$ [Figs. 5(c) and 5(d)] states but rather poor, in some instances, for the $o_3\,^1\Pi_u$ state [Figs. 6(a) and 6(b)]. For all of the $b\,^1\Pi_u$, $c_3\,^1\Pi_u$, and $o_3\,^1\Pi_u$ states, the present results clearly favor those of Khakoo *et al.* [14] over

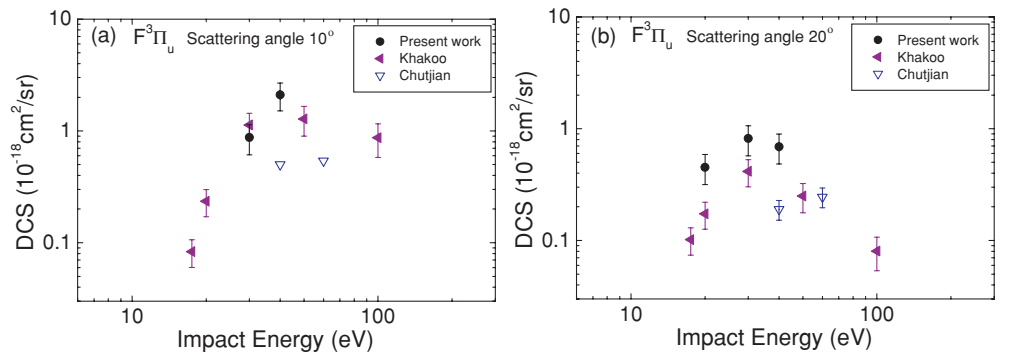

FIG. 8. (Color online) Energy dependence of the differential cross sections (10^{-18} cm^2/sr) for electron impact excitation of the $F\,^3\Pi_u$ electronic state in N_2. Present $F\,^3\Pi_u$ data (●) at (a) $\theta_{sc} = 10^\circ$ and (b) $\theta_{sc} = 20^\circ$ are compared to the earlier results of Khakoo *et al.* [14] (◀) and Chutjian *et al.* [9] (▽).

Chutjian *et al.* [9]. For both the $b'\,^1\Sigma_u^+$ [see Figs. 6(c) and 6(d)] and $c_4'\,^1\Sigma_u^+$ [see Figs. 7(a) and 7(b)] states, however, agreement between Khakoo *et al.* [14] and the current DCSs is quite poor with Khakoo *et al.* [14] seriously underestimating the cross-section magnitudes at each scattering angle and for both the excitation processes. On the other hand, for the $c_4'\,^1\Sigma_u^+$ [see Figs. 7(a), 7(b)], the data of Chutjian *et al.* [9] are in excellent accord with the results from our measurements. In Figs. 7(c) and 7(d), we again find excellent agreement between the present cross sections and those from Khakoo *et al.* [14], in this case for the electron impact excitation of the $G\,^3\Pi_u$ electronic state. A similar situation is also seen for the $F\,^3\Pi_u$ excitation function [see Fig. 8(a)] at $\theta_{sc} = 10^\circ$; however, at $\theta_{sc} = 20^\circ$ [Fig. 8(b)], the magnitudes of the DCSs from Khakoo *et al.* [14] are significantly lower than the present. All the excitation functions in Figs. 5–8 exhibit a very similar energy dependence. Namely, there is a strong rise in the magnitude of the cross sections from their respective thresholds up to a peak at an energy of about two to three times that threshold excitation energy; thereafter, the DCSs monotonically decrease in magnitude as the incident electron energy increases further. However, as the various measurements have all been taken on a rather coarse energy grid, the possibility of near-threshold resonances cannot be ruled out at this time.

IV. CONCLUSIONS

We have reported DCS measurements for 11 electronic states of N_2 in the energy-loss range 8.2–15.2 eV. The incident electron energies were 20, 30, and 40 eV and the scattered electron angles were 10° and 20°. For the $a\,^1\Pi_g$, $C\,^3\Pi_u$, $E\,^3\Sigma_g^+$, and $a''\,^1\Sigma_g^+$ states, where discrepancies do exist between the earlier data sets ([7–9,16,17] and references therein), the present results clearly favor the measured cross sections from the recent JPL/Fullerton collaboration [11,12,14,15] over those from the original JPL study [7–9] or from Brunger and Teubner [17]. This has clear ramifications for modeling of atmospheric phenomena, in which N_2 is a major constituent, such as on Earth and Titan, as both the $a\,^1\Pi_g$ and $C\,^3\Pi_u$ states are known [1–5] to play important roles either directly or via cascade. The present results also largely confirm the recent DCSs of Khakoo *et al.* [14] for the $b\,^1\Pi_u$, $c_3\,^1\Pi_u$, and $G\,^3\Pi_u$ electronic states; however, serious discrepancies (in a worst-case scenario up to a factor of 10) between our study and that of Khakoo *et al.* were noted, particularly at $\theta_{sc} = 20^\circ$, for the $o_3\,^1\Pi_u$, $b'\,^1\Sigma_u^+$, $c_4'\,^1\Sigma_u^+$, and $F\,^3\Pi_u$ electronic states. While the cross sections from Chutjian *et al.* [9] are in very good agreement with the present for the $c_4'\,^1\Sigma_u^+$ state, it is clear that further work, both experimental and theoretical, is required to resolve the remaining discrepancies for these latter four electronic states.

ACKNOWLEDGMENTS

This work was conducted under the support of the Japanese Ministry of Education, Sport, Culture and Technology. Additional support from the Australian Research Council, through its Centres of Excellence Program, is further noted. H.K. also acknowledges the Japan Society for the Promotion of Science for grants-in-aid for scientific research.

[1] L. Campbell, M. J. Brunger, P. J. O. Teubner, and D. C. Cartwright, J. Electron Spectrosc. Relat. Phenom. **144**, 119 (2005).
[2] L. Campbell, D. C. Cartwright, M. J. Brunger, and P. J. O. Teubner, J. Geophys. Res. **111**, A09317 (2006).
[3] L. Campbell, D. C. Cartwright, and M. J. Brunger, J. Geophys. Res. **112**, A08303 (2007).
[4] V. Degen, J. Geophys. Res. **87**, 10541 (1982).
[5] R. W. Eastes and W. E. Sharp, J. Geophys. Res. **92**, 10095 (1987).
[6] N. J. Mason, J. Phys. D **42**, 194003 (2009).
[7] D. C. Cartwright, A. Chutjian, S. Trajmar, and W. Williams, Phys. Rev. A **16**, 1013 (1977).
[8] D. C. Cartwright, S. Trajmar, A. Chutjian, and W. Williams, Phys. Rev. A **16**, 1041 (1977).
[9] A. Chutjian, D. C. Cartwright, and S. Trajmar, Phys. Rev. A **16**, 1052 (1977).
[10] S. Trajmar, D. F. Register, and A. Chutjian, Phys. Rep. **97**, 219 (1983).
[11] M. A. Khakoo, P. V. Johnson, I. Ozkay, P. Yan, S. Trajmar, and I. Kanik, Phys. Rev. A **71**, 062703 (2005).
[12] P. V. Johnson, C. P. Malone, I. Kanik, K. Tran, and M. A. Khakoo, J. Geophys. Res. **110**, A11311 (2005).
[13] M. A. Khakoo, S. Wang, R. Laher, P. V. Johnson, C. P. Malone, and I. Kanik, J. Phys. B **40**, F167 (2007).
[14] M. A. Khakoo, C. P. Malone, P. V. Johnson, B. R. Lewis, R. Laher, S. Wang, V. Swaminathan, D. Nuyujukian, and I. Kanik, Phys. Rev. A **77**, 012704 (2008).
[15] C. P. Malone, P. V. Johnson, I. Kanik, B. Ajdari, and M. A. Khakoo, Phys. Rev. A **79**, 032704 (2009).
[16] M. J. Brunger and S. J. Buckman, Phys. Rep. **357**, 215 (2002).
[17] M. J. Brunger and P. J. O. Teubner, Phys. Rev. A **41**, 1413 (1990).
[18] M. Allan, J. Phys. B **38**, 3655 (2005).
[19] R. F. da Costa and M. A. P. Lima, Int. J. Quantum Chem. **106**, 2664 (2006).
[20] R. F. da Costa and M. A. P. Lima, Phys. Rev. A **75**, 022705 (2007).
[21] M. Zubek and G. C. King, J. Phys. B **27**, 2613 (1994).
[22] H. Tanaka, T. Ishikawa, T. Masai, T. Sagara, L. Boesten, M. Takekawa, Y. Itikawa, and M. Kimura, Phys. Rev. A **57**, 1798 (1998).
[23] J. N. H. Brunt, G. C. King, and F. H. Read, J. Phys. B **10**, 1289 (1977).
[24] S. K. Srivastava, A. Chutjian, and S. Trajmar, J. Chem. Phys. **63**, 2659 (1975).
[25] L. Boesten and H. Tanaka, At. Data Nucl. Data Tables **52**, 25 (1992).
[26] H. Kato, H. Kawahara, M. Hoshino, H. Tanaka, M. J. Brunger, and Y.-K. Kim, J. Chem. Phys. **126**, 064307 (2007).

[27] L. Campbell, M. J. Brunger, P. J. O. Teubner, B. Mojarrabi, and D. C. Cartwright, Aust. J. Phys. **50**, 525 (1997).

[28] P. R. Bevington and D. K. Robinson, *Data Reduction and Error Analysis for the Physical Sciences* (McGraw-Hill, New York, 1992).

[29] F. R. Gilmore, R. R. Laher, and P. J. Espy, J. Phys. Chem. Ref. Data **21**, 1005 (1992).

[30] G. Joyez, R. I. Hall, J. Reinhardt, and J. Mazeau, J. Electron Spectrosc. Relat. Phenom. **2**, 183 (1973).

[31] D. Stahel, M. Leoni, and K. Dressler, J. Chem. Phys. **79**, 2541 (1983).